Citation for the original published paper:

Forsberg, S., Jonasson, E., De Sena, G., Temiz, I., Göteman, M. et al. (2025)
The impact of data time resolution on long-term voltage stability assessment: a case study with offshore wind-solar hybrid power plants
In: *14th Mediterranean Conference on Power Generation Transmission, Distribution and Energy Conversion (MEDPOWER 2024)* (pp. 767-772). Institution of Engineering and Technology
IET Conference Proceedings
https://doi.org/10.1049/icp.2024.4754

THE IMPACT OF DATA TIME RESOLUTION ON LONG-TERM VOLTAGE STABILITY ASSESSMENT: A CASE STUDY WITH OFFSHORE WIND-SOLAR HYBRID POWER PLANTS

Samuel Forsberg[1,2,*], Erik Jonasson[1], Geoffrey De Sena[1,2], Irina Temiz[1], Malin Göteman[1,2], Mikael Bergkvist[1,2]

[1]Department of Electrical Engineering, Uppsala University, Uppsala, Sweden
[2]Centre of Natural Hazards and Disaster Science, Uppsala, Sweden
**Samuel.forsberg@angstrom.uu.se*

Keywords: HYBRID POWER PLANTS, LONG-TERM VOLTAGE STABILITY, POWER GRID

Abstract

In this study, the impact of data time resolution on long-term voltage stability assessment of a power grid with high penetration of wind-solar hybrid power plants is investigated. Historical and synthetic wind data as well as solar irradiance are used to calculate power output from hypothetical offshore wind-solar hybrid power plants, geographically located off the coast of Massachusetts, USA. The results show that using hourly input data can overestimate the long-term voltage stability, compared with using minute data. However, the relative difference in terms of voltage mean value and standard deviation is marginal whilst the most significant difference is the intensity of the voltage fluctuations. The main drawback of using high-resolution data is the execution time, increasing proportionally with the number of time steps. Thus, it is argued that the choice of data time resolution should be based on the aspects of long-term voltage stability and the size of the power grid to be studied.

1 Introduction

Meeting greenhouse gas emission targets will require a rapid expansion of low-emission electricity generation. Renewable energy sources (RESs) such as wind farms and solar photovoltaics (PVs) can contribute significantly to this end. Recent decades have seen an exponential growth in onshore installations of both technologies, and the number of offshore wind farms (OWFs) is growing rapidly. The European Union aims to install at least 60 GW of offshore wind by 2030 [1]. However, this rapid increase in variable renewable electricity production poses a challenge to grid operators due to its intermittent nature. In the strive of reducing land space used by RESs and also decrease the power output variability, there has been recent interest in combining OWFs with floating PVs to form hybrid power plants (HPPs) [1].

In [2], the resilience to extreme storm events of power systems with large-scale offshore wind power generation was investigated. The resilience was quantified in terms of disconnected load, caused by power generating units shutting down due to wind exceeding the wind turbine's cut-out wind speed. The study shows that power systems with large-scale OWFs are highly vulnerable to extreme wind speeds, and that major blackouts can occur due to low voltages. The study was further developed in [3] where physical parameters affecting grids' resilience to storm conditions were identified and analysed. Power grid voltage stability with increasing RES penetration was investigated in [4], with the aim of evaluating a new stability index called critical voltage-reactive power ratio. Wind farms and PV parks were integrated in the power systems' models. The index was used to rank the buses according to the order in which RESs affect the voltage stability of the buses.

Time series simulations of energy system models are often based on hourly time steps. Among other things, this is due to the lack of high-resolution data [5]. When it comes to studies of RES integration into the power system, most available wind data are aggregated to a temporal resolution of 30 or 60 minutes [6]. However, to properly assess the reliability of power systems with high penetration of RES, high resolution data are necessary [5]. In this study, the impact of data time resolution on power system voltage stability assessment is quantified and analysed using statistical measures. Specifically, a power system with large-scale penetration of offshore wind-solar HPPs is investigated using hourly and minute geospatial weather data.

2 Methodology

2.1 Voltage stability

Dynamic voltage stability can be defined as the power system's ability to recover to an acceptable steady-state voltage at buses after being subjected to an external disturbance (e.g., changed weather conditions) [7]. A stable voltage level at all buses in a power grid is crucial for the successful operation of the grid. The lack of voltage stability can potentially lead to a voltage collapse that can cause power outages or even entire power system blackouts [8]. Dynamic voltage stability can be divided into short-term voltage stability (STVS) and long-term voltage stability (LTVS) [8], where LTVS refers to time scales of minutes [9].

In the present study, an LTVS approach is taken, focusing on voltage fluctuations on time scales of 1 minute and 1 hour, respectively. To study the voltage stability of the power grid, standard deviation, mean value, and quartile distance are used. The results in terms of voltage stability between simulations of 1 minute resolution are compared with simulations of 1 hour resolution.

2.2 Power system modelling and simulation

The IEEE39-bus model, also known as the New England power grid model, is used to investigate long-term voltage stability. The model consists of 39 buses interconnected with single line transmission lines. The IEEE39-bus model has been used extensively in previous research to perform resilience and stability analyses, see for example [2,10]. Quasi-dynamic simulations are performed using PowerFactory, developed by DigSilent. For each time step, power flow calculations are performed based on a full Newton-Raphson method, creating a dynamic behaviour based on static calculations. The balancing strategy for the power flow calculations is based on a method where the synchronous generators ramp up and down their power output to maintain the balance between power generation and demand at all time steps. If needed, generated power from the HPPs is curtailed to balance the grid.

In the model, the HPPs are locally controlled to keep the generator bus voltage as close as possible to a pre-defined setpoint of 1 pu. However, the generation and consumption of reactive power from the HPPs are limited to the capacity specified in predefined capability diagrams, limiting the voltage regulation capacity. Even though the characteristics of the capability diagram are simplified, they are designed to imitate the behaviour of real HPPs. The capability diagram used for the HPPs in the present study is shown in Fig. 1. The synchronous generators used the capability diagrams for conventional synchronous generators, as defined by DigSilent.

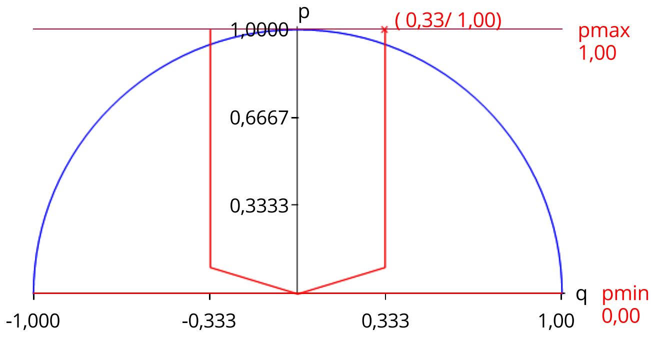

Fig. 1. Capability diagram for the HPPs.

In the modified New England model, two synchronous generators were replaced by HPPs at bus 33 and 35, which corresponds to a total HPP penetration of 16.5 %. The weather data coupled with the HPPs were recorded at the measurement sites QPTR1 (HPP connected to bus 33) and 44020 (HPP connected to bus 35), see Fig. 2.

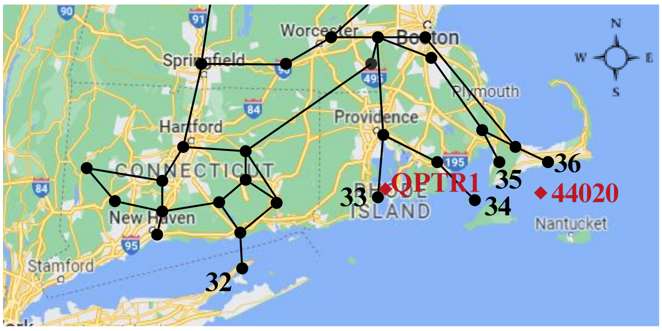

Fig. 2. Geographic representation of the New England model with measurement sites QPTR1 and 44020 marked. Map source: Google.

The installed capacities of the HPPs at bus 33 and 35 were set to three times larger than the steady-state power output from the synchronous generators at bus 33 and 35 in the original model. This was assumed based on the average capacity factor of offshore wind farms studied in [11].

Quasi-dynamic simulations of a period of a whole year were performed. More specifically, historical data from the year 2012 were used.

2.3 Wind and solar PV power

Synthetic minute resolved solar irradiance is generated using the Bright Solar Model, accessible at [12]. The model uses hourly weather observations to produce global irradiance at minute resolution via Markov chain processes. The development and full explanation of the model can be found in [13–17]. Hourly weather observations are taken from the reanalysis model ERA5 [18]. The power output from the solar PV is calculated as

$$P_{PV} = \eta \cdot A \cdot G \qquad (1)$$

where η is the panel efficiency, A is the panel area, and G is global horizontal irradiance.

The power output from the wind turbines is modelled using a multiturbine power curve, which is constructed as [19]

$$P_{mt}(v) = \int_{v-5}^{v+5} f(x|v,\sigma_u^2)P_{st}(x)dx \qquad (2)$$

where P_{mt} and P_{st} represent the power at wind speed v for a multi-turbine and a single-turbine power curve, respectively. The variance of the wind speeds within the park, σ_u^2, is assumed to be 1 m^2s^{-2}.

Wind speed data from the buoy QPTR1 off the coast of Massachusetts were available from [20] at 6 minute resolution. Histograms of the deviations from the 1 hour mean value were created. Using the maximum likelihood estimation function in MATLAB, Gaussian and Student's t-distributions were defined as done by [21]. A Laplacian distribution was manually defined as well. For each probability distribution, synthetic 6-minute wind speed data sets were generated for the location QPTR1 by pulling random values based on the probability distribution and adding them to each hourly mean value. Fig. 3 shows QQ-plots of the results from each distribution against the deviations in the measured data. Visual inspection indicated that Student's t-distribution leads to the nearest fit, the same conclusion reached by [21]. Then, this distribution was used to add stochastic fluctuations to the hourly wind data recorded at the 44020 site. To make the data compatible with the 1 minute insolation data, linear interpolation was used at both the QPTR1 and 44020 sites to define values between the 6-minute values.

The power output of the entire hybrid power plant P_{HPP} [pu] is the sum of the offshore wind power generation P_{OWF} [pu] and solar PV power generation P_{PV} [pu] at time step i calculated as

$$P_{HPP}(i) = \tfrac{1}{2}P_{OWF}(i) + \tfrac{1}{2}P_{PV}(i). \tag{3}$$

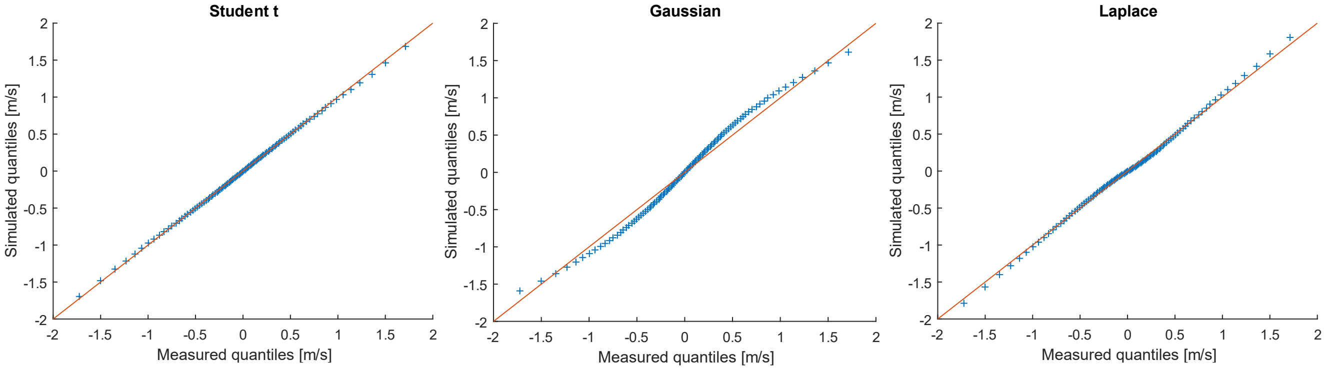

(a) (b) (c)

Fig. 3. QQ-plots of measured vs. simulated wind speed variation at location QPTR1 using (a) Student's t-, (b) Gaussian, and (c) Laplace distributions.

3 Results

A snapshot of the simulated voltages at bus 28 during June 1, 2012, is shown in Fig. 4. The voltage fluctuates strongly using 1 minute data compared with the usage of 1 hour data. A similar pattern can be observed at all other buses where the voltage deviates over time from the setpoint value of 1 pu.

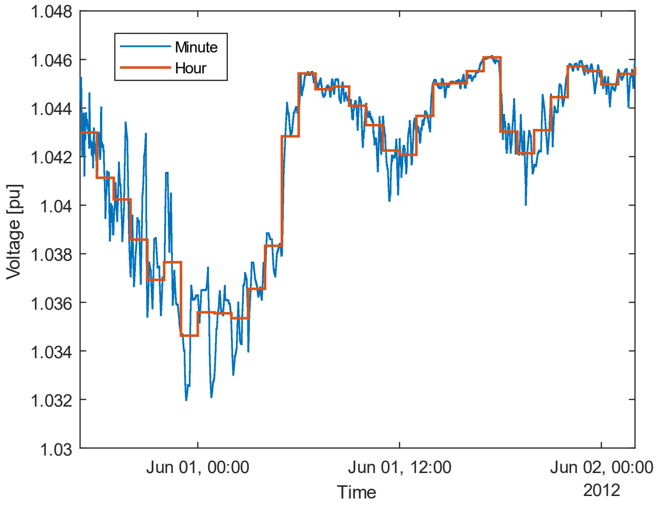

Fig. 4. Voltage levels at bus 28 during June 1, 2012, using hourly data and minute data.

From Fig. 5, the voltage standard deviations of buses 1-39 as observed during the year 2012 are shown. Consequently, the voltage standard deviation is higher for all buses with a non-zero standard deviation value when using 1 minute data compared with using 1 hour data. However, the deviation in terms of absolute value as well as the relative deviation differ from bus to bus.

The mean values of the voltages at buses 1-39 during the year 2012 are shown in Fig. 6. From the figure, it is seen that even though the voltages fluctuate more strongly using 1 minute data, the mean values are almost identical when comparing the results from 1 minute and 1 hour data resolution simulations.

A boxplot illustrating the voltage standard deviations at all buses using 1 minute and 1 hour data is shown in Fig. 7. As can be seen from the figure, the maximum value as well as the 75th percentile are higher in the case of 1 minute data, whilst the median, 25th percentile, and the minimum values are about the same in the two cases. This result is expected based on Fig. 5 and Fig. 6 and becomes clear considering the boxplot.

Information about simulation execution time and voltage data points generated are shown in Table 1. The simulations have been performed using a Windows laptop with 16 GB RAM, Intel Core i7-1185G7 processor, and an SSD hard drive.

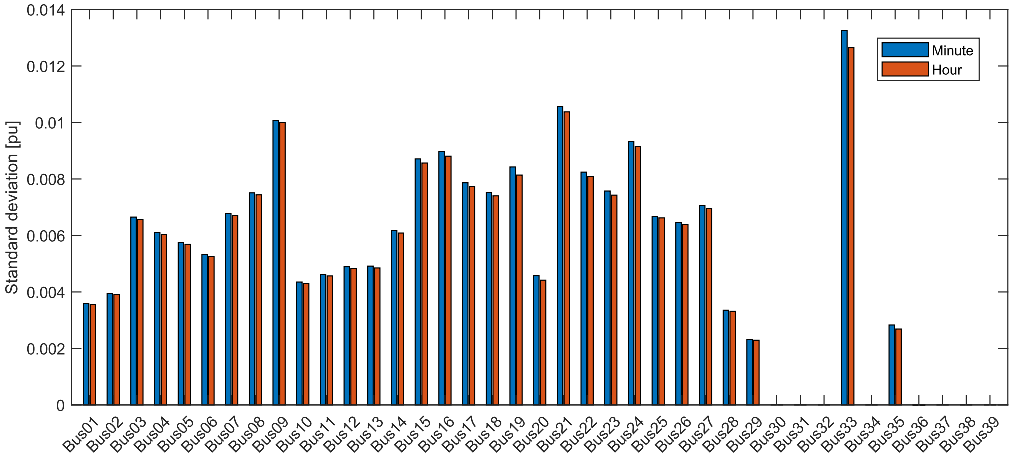

Fig. 5. Voltage standard deviations at bus 1-39 as observed during year 2012.

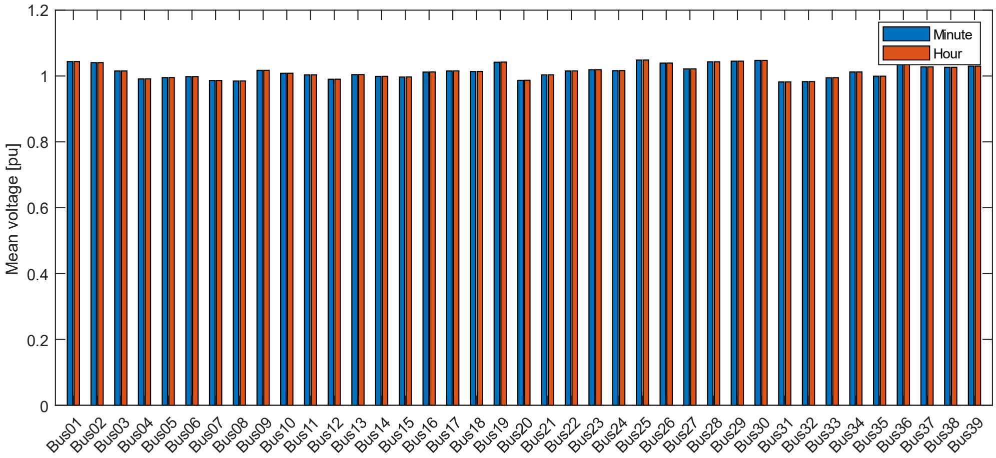

Fig. 6. Voltage mean values at bus 1-39 as observed during year 2012.

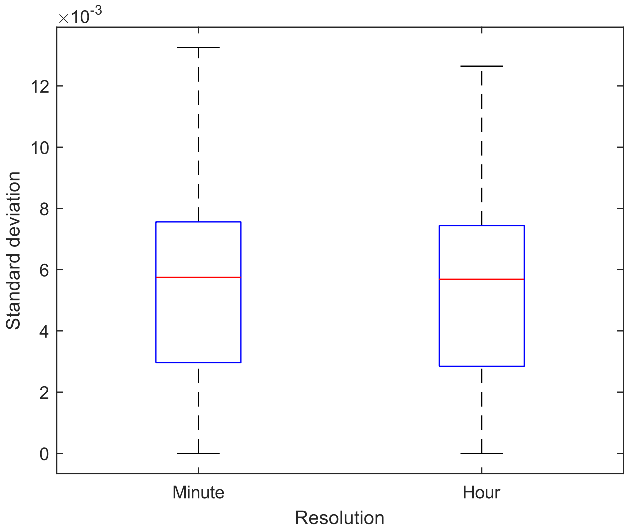

Fig. 7. Boxplot illustrating the standard deviations of the voltages at all 39 buses during a whole year.

Table 1. Overview of execution time and number of voltage data points in the case of 1 minute and 1 hour data resolution.

Data resolution	Execution time [min:s]	Voltage data points
Minute	24:47	20 554 560
Hour	00:25	342 576

4 Discussion

The results of the present study show that a data resolution of 1 minute consequently generates a higher voltage standard deviation compared with using a data resolution of 1 hour. Thus, using hourly wind and solar irradiation data is shown to overestimate the LTVS in power grids with high penetration of HPPs (or other RESs) compared with using 1 minute data resolution. However, even though the standard deviation differs in terms of magnitude between using 1 minute data and 1 hour data resolution, the boxplot in Fig. 7 shows that the relative difference is marginal. It should be noted that this is proved to be valid only for the investigated case. It is possible that factors such as the penetration of HPPs (or other RESs), physical grid structure, and time range of the quasi-dynamic simulations can affect the LTVS. A more thorough investigation of those and other parameters impact on LTVS is left for future studies.

The similarities in terms of voltage mean values at the different buses are expected since the random values used to create intra-hourly wind data were drawn from a symmetrical probability distribution function.

When the power generation fluctuates from the HPPs, the results show that the synchronous generators successfully manage to maintain the LTVS in the system. However, it is reasonable to assume that a higher penetration of HPPs (or other intermittent RESs) will make it more difficult for the synchronous generators to fully compensate for the power generation fluctuations. This could possibly affect the comparison of using 1 minute data and 1 hour data.

Statistical measures such as mean value and standard deviation are suitable for assessing the LTVS to some extent. However, none of these measures quantifies the intensity of the voltage fluctuations over time. From Fig. 4 it is obvious that using 1 minute data leads to a more strongly oscillating voltage profile, which is not successfully captured by any of the statistical measures used. Intensive voltage fluctuations put stress on real power systems and are therefore relevant to quantify when assessing the LTVS. Therefore, a further statistical analysis capturing the voltage oscillations is proposed for future research.

Even though high-resolution data can improve the accuracy in terms of LTVS assessment, the choice of data resolution should be considered as a trade-off between result accuracy and simulation execution time. From the present study, it is seen that the execution time is proportional to the number of simulation time steps. Simulating with 1 minute data instead of 1 hour data takes about 60 times longer and generates 60 times more voltage data points. For real power systems consisting of thousands of buses, assessing the LTVS will take significantly longer time. Thus, using a data resolution of 1 hour can in some cases be preferable to keep the execution time as short as possible, whilst still getting relatively accurate results. If the purpose by studying the LTVS is to assess the voltage mean value, a data time resolution of 1 hour seems preferable since it generates comparable results as simulations using 1 minute data. However, if intra-hourly voltage oscillations or voltage standard deviations are of interest for the LTVS assessment, 1 minute data is recommended.

5 Conclusion

The results from the LTVS assessments show that using hourly data overestimate the LTVS with respect to voltage standard deviation, as compared with using 1 minute data. However, the relative difference is small and therefore hourly data can in some cases be preferable to decrease execution time. If voltage oscillations are of interest when studying LTVS, a data resolution of 1 minute is proposed to capture the intra-hourly voltage fluctuations.

6 Acknowledgements

This work was funded by the Centre of Natural Hazards and Disaster Science (CNDS), STandUP for Energy, and the EU-SCORES project financed by the European Union’s Horizon 2020 and Green Deal Research and Innovation Programme under grant agreement No 101036457.

7 References

[1] European Commission. An EU Strategy to harness the potential of offshore renewable energy for a climate neutral future. Brussels: 2020.

[2] Forsberg S, Thomas K, Bergkvist M, Göteman M. Resilience to storm conditions of power systems with large dependencies on offshore wind. J Phys Conf Ser, Trondheim: 2023, p. 1–11. https://doi.org/10.1088/1742-6596/2626/1/012017.

[3] Forsberg S, Göteman M, Thomas K, Bergkvist M. Resilience to extreme storm conditions: A comparative study of two power systems with varying dependencies on offshore wind. Results in Engineering 2024;23:1–15. https://doi.org/10.1016/j.rineng.2024.102408.

[4] Adetokun BB, Maina Muriithi C, Ojo JO, Oghorada O. Impact assessment of increasing renewable energy penetration on voltage instability tendencies of power system buses using a QV-based index. Sci Rep 2023;13. https://doi.org/10.1038/s41598-023-36843-5.

[5] Omoyele O, Hoffmann M, Koivisto M, Larrañeta M, Weinand JM, Linßen J, et al. Increasing the resolution of solar and wind time series for energy system modeling: A review. Renewable and Sustainable Energy Reviews 2024;189:113792. https://doi.org/10.1016/J.RSER.2023.113792.

[6] Ward KR, Bamisile O, Ejiyi CJ, Staffell I. Time-averaged wind power data hides variability critical to renewables integration. Energy Strategy Reviews 2023;50:101235. https://doi.org/10.1016/J.ESR.2023.101235.

[7] Kundur P, Paserba J, Ajjarapu V, Andersson G, Bose A, Canizares C, et al. Definition and classification of power system stability. IEEE Transactions on Power Systems 2004;19:1387–401. https://doi.org/10.1109/TPWRS.2004.825981.

[8] Munkhchuluun E, Meegahapola L, Vahidnia A. Long-term voltage stability with large-scale solar-photovoltaic (PV) generation. International Journal of Electrical Power & Energy Systems 2020;117:105663. https://doi.org/10.1016/J.IJEPES.2019.105663.

[9] Löf A, Hill DJ, Arnborg S, Andersson G. On the analysis of long-term voltage stability. International Journal of Electrical Power & Energy Systems 1994;15:229–37. https://doi.org/doi.org/10.1016/0142-0615(93)90022-F.

[10] Jian Z, Guo J, Xu X. Optimal dispatch strategy analysis of fire extinguishing equipment for electric grid wildfire based on dynamic game. International Transactions on

Electrical Energy Systems 2020;30:1–17. https://doi.org/10.1002/2050-7038.12264.

[11] Crabtree CJ, Zappalá D, Hogg SI. Wind energy: UK experiences and offshore operational challenges. Proceedings of the Institution of Mechanical Engineers, Part A: Journal of Power and Energy 2015;229:727–46. https://doi.org/10.1177/0957650915597560.

[12] Bright JM. Bright Solar Model. GitHub 2018. https://jamiembright.github.io/BrightSolarModel/ (accessed April 11, 2024).

[13] Bright JM, Babacan O, Kleissl J, Taylor PG, Crook R. A synthetic, spatially decorrelating solar irradiance generator and application to a LV grid model with high PV penetration. Solar Energy 2017;147:83–98. https://doi.org/10.1016/J.SOLENER.2017.03.018.

[14] Smith CJ, Bright JM, Crook R. Cloud cover effect of clear-sky index distributions and differences between human and automatic cloud observations. Solar Energy 2017;144:10–21. https://doi.org/10.1016/J.SOLENER.2016.12.055.

[15] Bright JM, Taylor PG, Crook R. Methodology to stochastically generate synthetic 1-minute irradiance time-series derived from mean hourly weather observational data. ISES Solar World Congress 2015, Conference Proceedings, Daegu, South Korea: International Solar Energy Society; 2015, p. 142–51. https://doi.org/10.18086/swc.2015.07.02.

[16] Bright JM, Smith CJ, Taylor PG, Crook R. Stochastic generation of synthetic minutely irradiance time series derived from mean hourly weather observation data. Solar Energy 2015;115:229–42. https://doi.org/10.1016/J.SOLENER.2015.02.032.

[17] Bright JM, Bright JM, Taylor PG, Crook R. Methodology to Stochastically Generate Spatially Relevant 1-Minute Resolution Irradiance Time Series from mean Hourly Weather Data. 5th Solar Integration Workshop, Brussels, Belgium: 2015.

[18] Hersbach H, Bell B, Berrisford P, Biavati G, Horányi A, Muñoz Sabater J, et al. ERA5 monthly averaged data on single levels from 1940 to present. Copernicus Climate Change Service (C3S) Climate Data Store (CDS) 2024. https://doi.org/10.24381/cds.f17050d7.

[19] Olauson J, Bergkvist M. Modelling the Swedish wind power production using MERRA reanalysis data. Renew Energy 2015;76:717–25. https://doi.org/10.1016/j.renene.2014.11.085.

[20] National Oceanic and Atmospheric Administration. National Data Buoy Center n.d. https://www.ndbc.noaa.gov/ (accessed April 17, 2024).

[21] Murcia Leon JP, Koivisto MJ, Sørensen P, Magnant P. Power fluctuations in high-installation-density offshore wind fleets. Wind Energy Science 2021;6:461–76. https://doi.org/10.5194/WES-6-461-2021.